Earth **Surface**
Dynamics

Supplement of

Denudation rates across the Pamir based on ^{10}Be concentrations in fluvial sediments: dominance of topographic over climatic factors

M. C. Fuchs et al.

Correspondence to: M. C. Fuchs (fuchsm@mailserver.tu-freiberg.de)

1 Details on material and methods

1.1 Beryllium-10-based modern denudation rates

Beryllium-10 concentrations in modern fluvial sediments scale to the rate of landscape lowering by weathering and physical erosion and average the time of exposure to cosmic ray interaction in rock surfaces (von Blanckenburg, 2005; Dunai, 2010). The generally dry conditions in Pamir (Fig. **??**) suggest weathering to be of less importance in the total erosion budget. In this case, landscape lowering is dominated by the physical material removal at the landscape's surface, which means that denudation rates narrow down to erosion rates (e.g. Dunai, 2010), and it may be convenient to use both terms interchangeably in the following.

The relation between the ^{10}Be concentration in a target mineral and modern denudation rates is based on the fact that the nuclide is produced by cosmic rays at rock surfaces within a rock-characteristic attenuation depth, while material removal brings constantly new material from shielded depth to the surface (Lal, 1991; Brown et al., 1995; von Blanckenburg, 2005; Dunai, 2010). Being highest at the rock surface, the ^{10}Be production decreases approximately exponentially with depth (Lal, 1991; Dunne et al., 1999; Braucher et al., 2011). The mean attenuation path length z* of cosmic rays in rocks depends on the attenuation coefficient of the nucleonic component ($\sim$160 g/cm^2) and the rock density (e.g. Gosse and Phillips, 2001; Balco et al., 2008) of the bulk, often polymineral material. Accordingly, in silicate rocks z* is typically $\sim$60 cm (Lal, 1991; von Blanckenburg, 2005). The ^{10}Be concentration C is then proportional to the time the mineral grains reside within z* until being removed from the surface. Consequently, C is inversely proportional to the denudation rate ε (Lal, 1991; Brown et al., 1995; von Blanckenburg, 2005). This relation can be described by:

$$\varepsilon = \left(\frac{P}{C} - \lambda\right) * z^*$$ (1)

where λ is the decay constant of the nuclide and P its production rate. To calculate λ by

$$\lambda = \frac{ln(2)}{t_{1/2}}$$ (2)

we used the ^{10}Be half-life ($t_{1/2}$) of (1.387 ± 0.012) Ma (Korschinek et al., 2010). The parameter z* may be treated as a constant when determining basin-wide denudation rates that averages over local variations in rock densities affecting the attenuation path length. The central estimates required for solving the equation are the ^{10}Be concentration of the sample and the rate of nuclide production at the corresponding location (details given in sections **??**, 1.2 and 1.3). The equation is valid under steady-state conditions of ^{10}Be production and material removal at the surface. This implies constant conditions over a period that is long compared to the averaging time T_{ave}, the time it takes to erode z* and hence, to remove the 'cosmogenic memory' of the material (Brown et al., 1995; Bierman and Steig, 1996; von Blanckenburg, 2005; Dunai, 2010).

Assuming uniform erodibility, mineral composition and grain size release of the eroding rock surface, denudation rates represent averages for all upstream surfaces at the basin scale (Bierman and Steig, 1996; von Blanckenburg, 2005; Carretier et al., 2009). Well-mixed sediment representative of all process domains within the basin require sample basins large enough to minimize the influence of single and only local processes (e.g. von Blanckenburg, 2005; Niemi et al., 2005; Yanites et al., 2009). Although large basins imply longer grain travel times, nuclide concentrations revealed negligible increases compared to the concentration already acquired at their initial position in non-aggrading basins (Carretier et al., 2009).

1

1.2 Sample preparation and [10]Be measurements

The polymineral sediment samples required quartz enrichment before starting chemical cleaning and [10]Be extraction. To narrow the grain size fraction, we first sieved the samples to 250 - 500 μm and 500 - 1000 μm, and focussed on the 250 - 500 μm fraction. For two samples (TA28C and TA30P) only the coarser fraction yielded sufficient material. After magnetic separation and ultrasonic bath, we cleaned the quartz with a 1:1 solution of HCl (32%) and H_2SiF_6 (34%) (Brown et al., 1991). Inspection of the sample's mineral composition under the binocular revealed relatively high proportions of feldspars (up to 50%) for most of our samples, even after repeating the partial dissolution for six cycles. Feldspars cause bias in quartz results due to differing rates of [10]Be production. Additionally, the lower chemical resistance compared to quartz as well as high aluminum contents affect chemical procedures. This motivated us to introduce a standard feldspar flotation (Herber, 1969) to further enrich the quartz fraction. The feldspar flotation was carried out in a solution of 0.2% HF and pH of 2.4 - 2.7 to activate feldspar adherence to bubbles using the foam agent dodecylamine.

Atmospheric [10]Be was removed by dissolving 30% of the extracted quartz fraction with 48% HF during three cycles. The BeO separation followed the procedures by Merchel and Herpers (1999). After the addition of about 300 μg of a [9]Be carrier (Phena DD, $(3.025 \pm 0.009) \times 10^{-3}$ [9]Be/g, Merchel et al., 2008), samples were totally dissolved using 48% HF. The Be extraction from the dissolved quartz included repeated hydroxide precipitation by NH_{3aq}, anion and cation exchanges. For high Ti-containing samples, Ti was diminished by precipitation of $Ti(OH)_4$ before ignition of $Be(OH)_2$ to BeO. Then, target preparation involved adding Nb (six times of the dry oxide weight). AMS measurements were conducted at DREAMS (DREsden AMS, Helmholtz-Zentrum Dresden-Rossendorf, 6 MV, Cu cathode) using the in-house standard SMD-Be-12 (Akhmadaliev et al., 2013) normalized against the NIST SRM 4325 standard ([10]Be/[9]Be ratio of $(2.79 \pm 0.03) \times 10^{-11}$, Nishiizumi et al., 2007). A round-robin exercise of AMS facilities confirmed robust standard calibration and measurement configuration (Merchel et al., 2012). Processing blanks were treated and measured parallel to the sediment samples. The blank isotope ratios in the order of 0.3 - 1.7% ([10]Be/[9]Be ratio of 2.0×10^{-15} and 2.1×10^{-15}) were subtracted from the measured ratios of all samples.

1.3 Production rates and shielding factor

The production of [10]Be in quartz is primarily dependent on the cosmogenic particle flux from nucleons and muons (Lal, 1991; Granger and Muzikar, 2001) as a function of the geomagnetic field, altitude and shielding (Lal, 1991; Brown et al., 1995; Bierman and Steig, 1996; Stone, 2000; Gosse and Phillips, 2001). Accounting for the location-specific modulation, reference sea level and high latitude (SLHL) production rates need to be scaled to the conditions at the site of sampling.

In the case of fluvial sediment samples, the cosmogenic nuclide inventory was acquired in source areas of the sediment upstream of the sampled site (e.g. Brown et al., 1995; Bierman and Steig, 1996; Granger et al., 1996; von Blanckenburg, 2005). Consequently, the calculation of representative production rates requires attention to the hypsometry of the whole basin (von Blanckenburg, 2005; Norton and Vanacker, 2009; Dunai, 2010). Representative values for the production rate and shielding were calculated raster-cell resolved for the upstream area of each sampling site based on a ASTER GDEM of 10 m resolution (see also main text).

For each sampled basin, we then calculated [10]Be production rates from neutrons, and fast and stopped muons by raster cell-resolved scaling of a SLHL reference according to (Stone, 2000). We used the SLHL production rate of 4.5 at/g quartz/yr (cf. Balco et al. 2008 along with the half-life of [10]Be of $(1.387 \pm 0.012) \times 10^6$ years, Korschinek et al. 2010) and the attenuation parameters according to Braucher et al. (2003) and Siame et al. (2004).

Topographic shielding plays an important role in high relief terrain (Dunne et al., 1999) as steep slopes reduce the exposure to the cosmic particle flux (e.g. Gosse and Phillips, 2001; Codilean, 2006; Norton and Vanacker, 2009). Shielding from other sources is considered negligible as glaciated areas are excluded from production rate calculation and vegetation is scarce due to the dry climate and high

basin altitudes. The shielding factor was estimated for each GDEM raster cell based on the horizon line within a 10 km distance according to the method of Codilean (2006). Norton and Vanacker (2009) found only low underestimation of shielding when using a DEM of 30 m resolution in steep terrain.

95 ## 2 Details on results

2.1 Details on denudation rate parameters

Denudation rates corrected for the basins proportion of snow and ice cover display an exponential relation with AMS-based [10]Be concentrations (Fig. S2, B) as an expression of the attenuation of cosmic rays in rock surfaces.

100 The correction of production rates according to the basin's topographic shielding factors enhance differences between basins. Low altitude areas commonly relate to marginal Pamir basins that are more shielded by steep slopes than plateau-related basins with a high proportion of altitudes above 3600 m a.s.l. and large areas of slopes <5%. Consequently, elevated central and eastern basin portions deliver sediments of high [10]Be concentrations (e.g., TA08N) to the river channels due to
105 high production and low shielding. Lowest production rates occur within north-western basins (e.g. TA02A) due to both, high topographic shielding and high snow and ice cover. The rates of nuclide production (Tab. **??**) are similar, with only ∼9% variability for plateau-related basins (TA08N and TA30P) and those of the southern Panj basins (TA23P, TA24O, TA25C and TA28C). The shielding corrected production rates in tributary basins indicate a slight decrease (Fig. S2 in supplementary
110 material, C) corresponding to northward lower altitudes and steepened topography.

3 Supplementary figures

3.1 Figure S1: Spatial variations of ^{10}Be production rates and topographic shielding
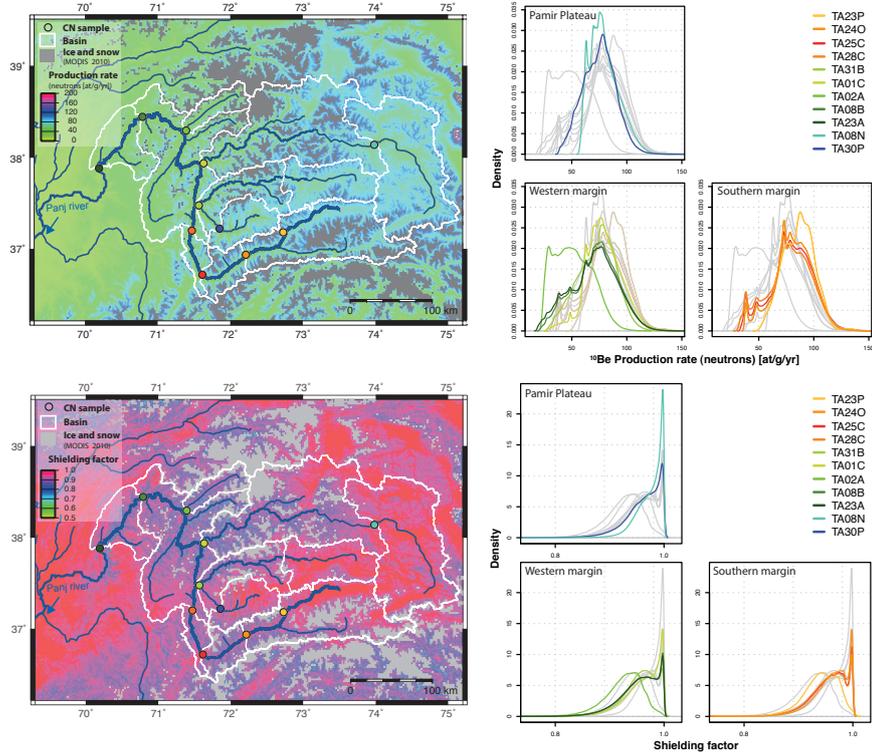
Figure S1. Spatial variations of ^{10}Be production rates and topographic shielding according to the hypsometry of the Pamir, and individual frequency distributions of production and shielding within sampled basins (cf. Figs. 1 and 2). As an example of the spatially variable production, rates are given for the neutron induced ^{10}Be built-up (CN: cosmogenic nuclide, color code for CN sample locations in map refers to individual basins in the legend of frequency distribution plots: reddish: southern Pamir margin, greenish: western Pamir margin, blueish: plateau-related basins, cf. Fig. 1; notation of basins refers to bold fonts used for sample names in Fig. 1 and Tab. 1).

3.2 Figure S2: Parameters of denudation rate calculations
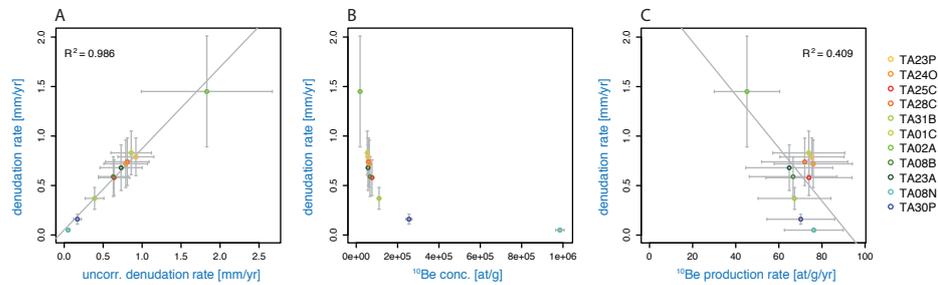
Figure S2. Relationship between basin-wide denudation rates and respective parameters used for calculations and corrections. A: Denudation rates with and without correction for areas covered by permanent snow and ice. B: Exponential relation between denudation and ^{10}Be concentrations from AMS measurements. C: Low variability of production rates corrected for topographic shielding (color code refers to individual basins in the legend, reddish: southern Pamir margin, greenish: western Pamir margin, blueish: plateau-related basins, cf. Fig. 1; notation of basins refers to bold fonts used for sample names in Fig. 1 and Tab. 1, shaded areas provide a quick demarcation of margin or plateau-related samples, the sample TA01C between the two units illustrates the integration of both, marginal and plateau-related portions).

References

115 Akhmadaliev, S., Heller, R., Hanf, D., Rugel, G., and Merchel, S.: The new 6 MV AMS-facility DREAMS at Dresden, Nuclear Inst. and Methods in Physics Research, B, 294, 5–10, 2013.

Balco, G., Stone, J. O., Lifton, N. A., and Dunai, T. J.: A complete and easily accessible means of calculating surface exposure ages or erosion rates from ^{10}Be and ^{26}Al measurements, Quaternary Geochronology, 3, 174–195, 2008.

120 Bierman, P. R. and Steig, E. J.: Estimating rates of denudation using cosmogenic isotope abundances in sediment, Earth Surface Processes and Landforms, 21, 125–139, 1996.

Braucher, R., Brown, E. T., Bourlès, D. L., and Colin, F.: In situ produced ^{10}Be measurements at great depths: implications for production rates by fast muons, Earth and Planetary Science Letters, 211, 251–258, 2003.

Braucher, R., Merchel, S., Borgomano, J., and Bourlès, D. L.: Production of cosmogenic radionuclides at great

125 depth: A multi element approach, Earth and Planetary Science Letters, 309, 1–9, 2011.

Brown, E. T., Edmond, J. M., Raisbeck, G. M., Yiou, F., Kurz, M. D., and Brook, E. J.: Examination of surface exposure ages of Antarctic moraines using *in situ* produced ^{10}Be and ^{26}Al, Geochimica et Cosmochimica Acta, 55, 2269–2283, 1991.

Brown, E. T., Stallard, R. F., Larsen, M. C., Raisbeck, G. M., and Yiou, F.: Denudation rates determined from the

130 accumulation of in situ-produced ^{10}Be in the Luquillo Experimental Forest, Puerto Rico, Earth and Planetary Science Letters, 129, 193–202, 1995.

Carretier, S., Regard, V., and Soual, C.: Theoretical cosmogenic nuclide concentration in river bed load clasts: Does it depend on clast size?, Quaternary Geochronology, 4, 108–123, 2009.

Codilean, A. T.: Calculation of the cosmogenic nuclide production topographic shielding scaling factor for large

135 areas using DEMs, Earth Surface Processes and Landforms, 31, 785–794, 2006.

Dunai, T.: Cosmogenic Nuclides: Principles, Concepts and Applications in the Earth Surface Sciences., Cambridge, 2010.

Dunne, J., Elmore, D., and Muzikar, P.: Scaling factors for the rates of production of cosmogenic nuclides for geometric shielding and attenuation at depth on sloped surfaces, Geomorphology, 27, 3–11, 1999.

140 Gosse, J. C. and Phillips, F. M.: Terrestrial in situ cosmogenic nuclides: Theory and application, Quaternary Science Reviews, 20, 1475–1560, 2001.

Granger, D. E. and Muzikar, P. F.: Dating sediment burial with in situ-produced cosmogenic nuclides: Theory, techniques, and limitations, Earth and Planetary Science Letters, 188, 269–281, 2001.

Granger, D. E., Kirchner, J. W., and Finkel, R.: Spatial averaged long-term erosion rates measured from in

145 situ-produced cosmogenic nuclides in alluvial sediment, Journal of Geology, 104, 249–257, 1996.

Herber, L. J.: Separation of feldspar from quartz by flotation, The American Mineralogist, 54, 1212–1215, 1969.

Korschinek, G., Bergmaier, A., Faestermann, T., Gerstmann, U. C., Knie, K., Rugel, G., Wallner, A., Dillmann, I., Dollinger, G., von Gostomski, C. L., Kossert, K., Maiti, M., Poutivtsev, M., and Remmert, A.: A new value for the half-life of ^{10}Be by Heavy-Ion Elastic Recoil Detection and liquid scintillation counting, Nuclear Inst.

150 and Methods in Physics Research, B, 268, 187–191, 2010.

Lal, D.: Cosmic ray labeling of erosion surfaces: *in situ* nuclide production rates and erosion models, Earth and Planetary Science Letters, 104, 424–439, 1991.

Merchel, S. and Herpers, U.: An update on radiochemical separation techniques for the determination of long-lived radionuclides via accelerator mass spectrometry, Radiochim. Acta, 84, 215–219, 1999.

155 Merchel, S., Arnold, M., Aumaître, G., Benedetti, L., Bourlès, D. L., Braucher, R., Alfimov, V., Freeman, S. P. H. T., Steier, P., and Wallner, A.: Towards more precise ^{10}Be and ^{36}Cl data from measurements at the 10^{14} level: Influence of sample preparation, Nuclear Inst. and Methods in Physics Research, B, 266, 4921–4926, 2008.

Merchel, S., Bremser, W., Akhmadaliev, S., Arnold, M., Aumaître, G., Bourlès, D. L., Braucher, R., Caffee, M.,

160 Christl, M., Fifield, L. K., Finkel, R. C., Freeman, S. P. H. T., Ruiz-Gómez, A., Kubik, P. W., Martschini, M., Rood, D. H., Tims, S. G., Wallner, A., Wilcken, K. M., and Xu, S.: Quality assurance in accelerator mass spectrometry: Results from an international round-robin exercise for ^{10}Be, Nuclear Inst. and Methods in Physics Research, B, 289, 68–73, 2012.

Niemi, N. A., Oskin, M., Burbank, D. W., Heimsath, A. M., and Gabet, E. J.: Effects of bedrock land-

165 slides on cosmogenically determined erosion rates, Earth and Planetary Science Letters, 237, 480 – 498, doi:http://dx.doi.org/10.1016/j.epsl.2005.07.009, 2005.

Nishiizumi, K., Imamura, M., Caffee, M. W., Southon, J. R., Finkel, R. C., and McAninch, J.: Absolute calibration of ^{10}Be AMS standards, Nuclear Instruments and Methods in Physics Research, B, 258, 403–413, 2007.

170 Norton, K. P. and Vanacker, V.: Effects of terrain smoothing on topographic shielding correction factors for cosmogenic nuclide-derived estimates of basin-averaged denudation rates, Earth Surface Processes and Landforms, 34, 145–154, 2009.

  Siame, L., Bellier, O., Braucher, R., Sébrier, M., Cushing, M., Bourlès, D., Hamelin, B., Baroux, E., de Voogd, B., Raisbeck, G., and Yiou, F.: Local erosion rates versus active tectonics: cosmic ray exposure modelling in

175 Provence (south-east France), Earth and Planetary Science Letters, 220, 345–364, 2004.

  Stone, J. O.: Air pressure and cosmogenic isotope production, Journal of Geophysical Research: Solid Earth, 105, 23 753–23 759, 2000.

  von Blanckenburg, F.: The control mechanisms of erosion and weathering at basin scale from cosmogenic nuclides in river sediment, Earth and Planetary Science Letters, 237, 462–479, 2005.

180 Yanites, B. J., Tucker, G. E., and Anderson, R. S.: Numerical and analytical models of cosmogenic radionuclide dynamics in landslide-dominated drainage basins, J. Geophys. Res., 114, F01 007, doi:10.1029/2008JF001088, 2009.